

Functional screening identifies miR-315 as a potent activator of Wingless signaling

Serena J. Silver*, Joshua W. Hagen†, Katsutomo Okamura†, Norbert Perrimon**‡, and Eric C. Lai†*

*Department of Genetics, Howard Hughes Medical Institute, Harvard Medical School, 77 Avenue Louis Pasteur, Boston, MA 02115; and †Department of Developmental Biology, Sloan-Kettering Institute, 1275 York Avenue, Box 252, New York, NY 10021

Edited by Stephen J. Elledge, Harvard Medical School, Boston, MA, and approved September 20, 2007 (received for review July 16, 2007)

The existence of vast regulatory networks mediated by microRNAs (miRNAs) suggests broad potential for miRNA dysfunction to contribute to disease. However, relatively few miRNA–target interactions are likely to make detectable contributions to phenotype, and effective strategies to identify these few interactions are currently wanting. We hypothesized that signaling cascades represent critical points of susceptibility to miRNA dysfunction, and we developed a strategy to test this theory by using quantitative cell-based screens. Here we report a screen for miRNAs that affect the Wingless (Wg) pathway, a conserved pathway that regulates growth and tissue specification. This process identified ectopic miR-315 as a potent and specific activator of Wg signaling, an activity that we corroborated in transgenic animals. This miR-315 activity was mediated by direct inhibition of *Axin* and *Notum*, which encode essential, negatively acting components of the Wg pathway. Genetic interaction tests substantiated both of these genes as key functional targets of miR-315. The ability of ectopic miR-315 to activate Wg signaling was not a trivial consequence of predicted miRNA–target relationships because other miRNAs with conserved sites in the *Axin* 3' UTR neither activated Wg outputs nor inhibited an *Axin* sensor. In summary, activity-based screening can selectively identify miRNAs whose deregulation can lead to interpretable phenotypic consequences.

microRNA | signal transduction

MicroRNAs (miRNAs), a large class of ≈ 22 -nt noncoding RNA, mediate extensive gene-regulatory networks whose functional implications are only beginning to be understood (1). Computational studies indicate that a substantial proportion of cellular transcripts are directly regulated by miRNAs (2). Thus, almost any biological process of choice may be plausibly considered to be under miRNA-mediated control. However, few miRNAs are functionally well understood at present. Because individual miRNAs are often predicted to have hundreds of potential targets, it is difficult to decide *a priori* that any given miRNA–target interaction is particularly meaningful.

The need to identify phenotypically relevant activities and targets of animal miRNAs stems from the finding that miRNA dysfunction is causal to disease and oncogenesis. For example, let-7 family members have been suggested to serve as tumor suppressors by directly inhibiting the *Hmg2A* and *RAS* protooncogenes (3–6). Conversely, the related miR-372/373 miRNAs promote tumorigenesis in combination with oncogenic RAS, at least in part by directly inhibiting the tumor suppressor *LATS2* (7). Likewise, the miR-17–92 cluster (8, 9) synergizes with MYC to induce B cell lymphoma.

Because many diseases and cancers are due to the perturbation of dose-sensitive signal-transduction cascades that control cell growth and differentiation, we hypothesized that such pathways provide fertile ground for mining the disease-relevant activities of miRNAs. Indeed, a growing body of work demonstrates biologically important roles for specific miRNAs in regulating the major signaling cascades. For example, aspects of Hedgehog signaling are regulated by miR-214 in zebrafish (10), whereas many components of the *Drosophila* Notch pathway are regulated by Brd box-, GY box-, and/or K box-family miRNAs (11–13). Therefore, we devel-

oped a functional screening approach to examine the ability of miRNAs to modulate the transcriptional outputs of signal-transduction cascades. In this report, we used the Wingless (Wg)–Wnt pathway as a testbed for our approach.

The *Drosophila* morphogen Wg and its vertebrate homologs (Wnts) coordinate a conserved signaling system that directs cell specification, tissue patterning, and cell proliferation. Because precise levels of the Wg–Wnt pathway output are essential for appropriate biological outcomes, net pathway output is carefully balanced by the interplay of positive and negative factors. In fact, Wg–Wnt signaling is modulated at almost every conceivable level, from transcriptional regulation to posttranslational modifications, including lipidation, glycosylation, phosphorylation, and ubiquitination (14). The need to maintain tight control over this pathway is reflected by the fact that inappropriate Wnt pathway activity underlies developmental disorder and disease, including liver, colorectal, breast, and skin cancer (14).

We generated a library of miRNA expression constructs and analyzed their effects on a quantitative Wg reporter assay in *Drosophila* cells (15). Our approach identified miR-315 as a potent activator of Wg signaling in cultured cells, an activity that we confirmed in transgenic animals. We determined that miR-315 activates Wg signaling by independently repressing two negative regulators of Wg signaling, *Axin* and *Notum*. Notably, a specific connection between miR-315 and Wg signaling could not have been anticipated from the outset by inspection of the >400 predicted, conserved targets of miR-315. Our validated strategy for investigating the influence of miRNA gain of function on signaling pathways suggests that this approach efficiently elucidates disease-relevant activities of human miRNAs.

Results

A Plasmid-Based miRNA Expression Library for Use in Cell-Based Assays. Although bioinformatics has yielded important insights into miRNA biology, miRNA target lists alone are of limited utility in assigning miRNA function. This finding is partly because of the large number of targets predicted for most miRNAs (often 50–200). For example, in the Wg pathway alone, ≈ 60 miRNA–mRNA target predictions are made by various algorithms (16–18) [supporting information (SI) Table 1]. Additional concerns surround the functional significance of many

Author contributions: S.J.S. and J.W.H. contributed equally to this work; S.J.S., J.W.H., and E.C.L. designed research; S.J.S., J.W.H., K.O., and E.C.L. performed research; E.C.L. contributed new reagents/analytic tools; S.J.S., J.W.H., N.P., and E.C.L. analyzed data; and S.J.S. and E.C.L. wrote the paper.

The authors declare no conflict of interest.

This article is a PNAS Direct Submission.

Freely available online through the PNAS open access option.

Abbreviations: DRSC, *Drosophila* RNAi Screening Center; miRNA, microRNA; TCF, T cell factor.

†To whom correspondence may be addressed. E-mail: perrimon@receptor.med.harvard.edu or laie@mskcc.org.

This article contains supporting information online at www.pnas.org/cgi/content/full/0706673104/DC1.

© 2007 by The National Academy of Sciences of the USA

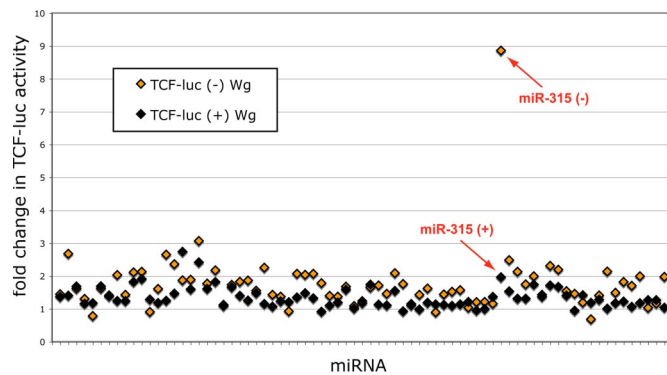


Fig. 1. Genome-wide cell-based screen for miRNAs identifies miR-315 as an activator of Wg signaling in unstimulated cells. Naive (–) cells or Wg-expressing (+) clone 8 cells were transfected with individual UAS-DsRed-miRNA expression plasmids, ub-Gal4 activator plasmid, TCF-luc (firefly), and pol III-luc (*Renilla*) reporters. Modification of Wg pathway activity was monitored by changes in the expression of TCF-luc relative to the control pol III-luc reporter. Wg (–) screen data are reported in orange, whereas Wg (+) screen data are reported in black. Both data sets were normalized by setting the TCF-luc:pol III-luc ratio in the presence of ub-Gal4 and UAS-DsRed to 1. The complete primary data are reported in [SI Table 2](#).

computationally predicted miRNA–target interactions, as well as the extent to which noncanonical targets might be missed by the major computational approaches (2, 19, 20).

To move away from target-motivated hypotheses in favor of activity-based tests of miRNA function, we took advantage of a robust transcriptional reporter for Wg signaling in *Drosophila* clone 8 cells (15). The Wg signal is transduced by the T cell factor (TCF) family of transcription factors whose activation can be quantified by a firefly luciferase reporter linked to multiple TCF-binding sites (TCF-luc) (21). Although this reporter does not capture all aspects of Wg signaling *in vivo* (22), TCF-luc is nonetheless a useful monitor of experimental perturbations to Wg signal transduction in cultured cells.

To examine the effect of ectopic miRNAs on TCF-luc, we chose a pri-miRNA expression strategy previously shown to produce active miRNAs in transgenic animals (23). We cloned 400- to 500-nt pri-miRNA fragments centered on the miRNA hairpin into the 3' UTR of pUAST or UAS-DsRed vectors. This library includes 77/78 miRNA loci currently deposited in miR-Base (24), with some miRNAs represented as both single constructs and members of multigene operons (see [SI Table 2](#) for a list of the 75 miRNA expression constructs). Analysis of many such constructs *in vivo* indicates that the Gal4>UAS-miRNA strategy does not saturate the endogenous miRNA biogenesis or regulatory pathways (13, 23). miRNA expression was induced by cotransfection of a plasmid encoding constitutively expressed Gal4 (*ub-Gal4*), and Wg pathway activity was measured as the ratio of TCF-luc to a pol III-*Renilla* luciferase control. Because Wg signaling is actively repressed in unstimulated cells, we performed these assays in naive clone 8 cells, as well as in cells transfected with a Wg expression construct (pAc-Wg) (15).

Expression of miR-315 Strongly Stimulates Basal Wg Pathway Activity.

Most miRNAs failed to alter TCF-luc activity >2-fold in either resting or Wg-stimulated conditions (Fig. 1 and [SI Table 2](#)). Of those miRNAs that did, miR-315 caused the most striking change in Wg pathway activity, inducing a 9-fold increase in TCF-luc in the absence of Wg (Fig. 1). Interestingly, although miR-315 caused the third highest increase in TCF-luc activity in the presence of Wg, its effect there was comparatively modest (2-fold induction). Therefore, miR-315 predominantly activated Wg signaling in otherwise unstimulated clone 8 cells.

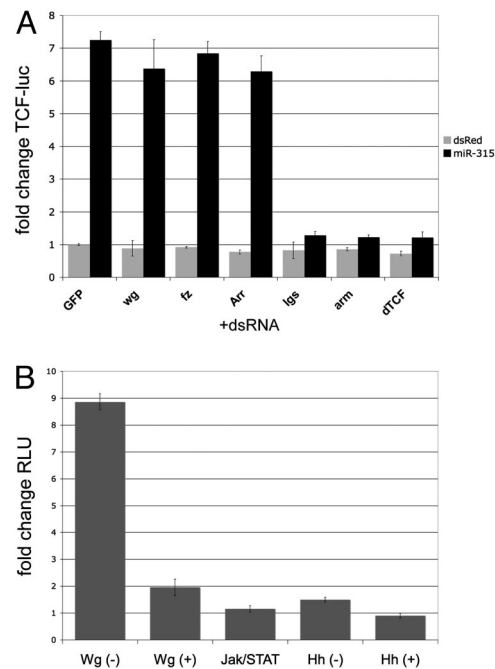


Fig. 2. Placement and specificity of miR-315 activity relative to the Wg pathway. (A) Epistasis test. The effect of ectopic miR-315 on TCF-luc was determined in the presence of dsRNAs against various positive components of the canonical Wg signaling pathway. In clone 8 cells, miR-315 acts downstream of the Wg ligand and its receptors (Fz and Arr) but upstream of the nuclear components legless, Arm, and dTCF. (B) Specificity test. miR-315 had no effect on a reporter for transcriptional output of the JAK/STAT pathway (10X-STAT92-luc) and no effect on a reporter for transcriptional output of the Hedgehog (Hh) pathway (*ptcΔ136-luc*) under either Hh-stimulated or unstimulated conditions. RLU, relative luciferase units for the various reporters.

To determine where in the Wg pathway miR-315 acts, we performed epistasis tests that asked whether miR-315 could activate TCF-luc after dsRNA-mediated knockdown of various positive components of the Wg pathway. miR-315 induced TCF-luc independently of the Wg ligand, the frizzled receptor, or the LRP/arrow coreceptor, but required the function of the nuclear factors legless/BCL9, pangolin/dTCF, and armadillo/ β -catenin (Fig. 2A). These data placed miR-315 activity in cultured cells downstream of the plasma membrane-localized Wg receptors, but upstream of the nuclear components of this signaling pathway.

We assessed the specificity of miR-315 activity by using transcriptional reporters for other signaling pathways. We found that miR-315 did not affect a reporter for JAK-STAT signaling and had no effect on a reporter for Hedgehog signaling under either basal or stimulated conditions (Fig. 2B). These data, in combination with the epistasis test with Wg pathway nuclear factors, exclude that ectopic miR-315 operates nonspecifically by some general inhibitor of the basal transcriptional machinery. Finally, we attempted to perform reciprocal experiments to knockdown miR-315 by using 2'-*O*-methylated antisense oligonucleotides (25), but observed no effect on either Wg (–) or Wg (+) conditions. Subsequent miRNA microarray studies showed that miR-315 is not expressed by any commonly used *Drosophila* tissue culture cells (clone 8, S2, or Kc cells) (data not shown). Therefore, we could not perform complementary inhibitor studies. Instead, we turned to *in vivo* animal assays to further probe the functional relationship between miR-315 and the Wg pathway.

miR-315 Activates Wg Signaling in Transgenic Animals. The induction of a Wg-responsive reporter in cultured cells by miR-315 does

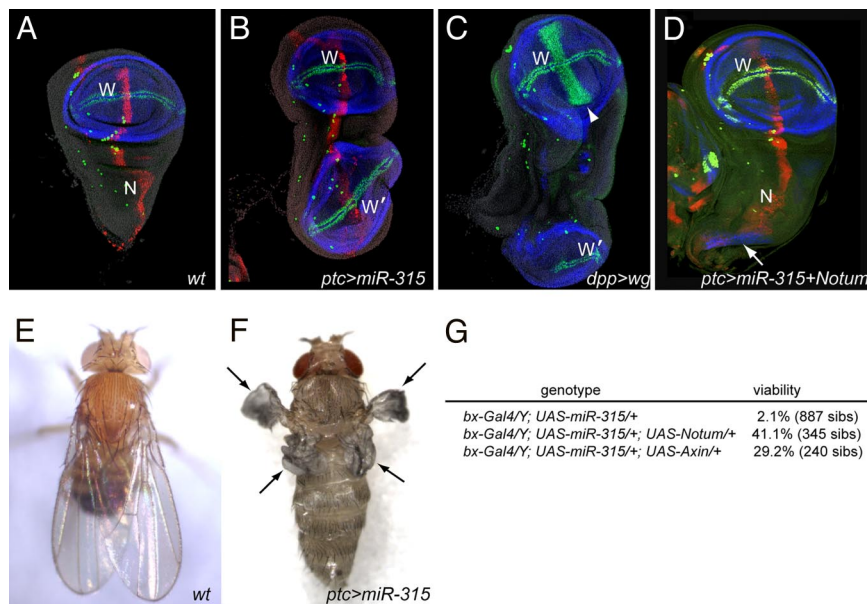


Fig. 3. miR-315 is a potent activator of Wg signaling *in vivo*. (A) Wild-type third instar wing imaginal disk expressing DsRed under the control of *ptc-Gal4*. W, presumptive wing; n, presumptive notum. Disk was stained for Nubbin (in blue) to mark the wing pouch and Sens (in green) to mark cells that flank the wing margin. Sens also is expressed by sensory organ precursor cells located along the anterior wing margin and the presumptive notum. (B) *ptc-Gal4, UAS-DsRed-miR-315* disk exhibits complete transformation of the notum into a second wing pouch (W'). (C) *dpp-Gal4, UAS-wg* animals display a similar notum-wing transformation; *dpp-Gal4* was used here as expression of Wg by using *ptc-Gal4*, which was lethal at earlier stages. Wg also induces ectopic sensory organs in the normal wing pouch, resulting in a band of Sens-positive cells perpendicular to the endogenous wing margin (arrowhead). (D) *ptc-Gal4, UAS-DsRed-miR-315, UAS-Notum* wing disk exhibits suppressed wing transformation, although a remnant of Nubbin⁺ tissue can be seen in the notal region (arrow). (E) Wild-type adult fly. (F) Although mostly lethal at earlier stages, *ptc-Gal4, UAS-DsRed-miR-315* pharate survivor displays prominent transformation of the scutellar region of the notum into ectopic wings (arrows). The premature death of these animals precludes normal inflation of their wings. (G) Rescue of *bx-Gal4>miR-315*-induced lethality by coexpressed *Axin* and *Notum*. The viability of these genotypes was determined as a percentage of their control balanced siblings from the same crosses.

not necessarily mean that it can affect Wg signaling in an interpretable manner in the animal. For example, miR-315 might regulate other targets that could together induce confounding phenotypes. Indeed, with hundreds of targets predicted for individual miRNAs (including miR-315), computational studies do not readily predict interpretable consequences for deregulating individual miRNAs. Therefore, we analyzed the consequences of ectopic miR-315 on *Drosophila* development by using stably integrated *UAS-DsRed-miR-315* transgenes.

Patterning of the wing imaginal disk is a well established model system for studying many fundamental cell-signaling pathways, including the Wg pathway. Each of the two wing imaginal discs gives rise to one half of the notum, or back of the fly, and to one of the adult wings. The domain that gives rise to the wing, or wing pouch, can be visualized by expression of Nubbin (Fig. 3A, blue cells). This domain is bisected by a line of Cut-expressing cells termed the “wing margin.” These cells induce the expression of Senseless (Sens) in two flanking rows of cells that include the precursors for sensory organs of the anterior wing margin (Fig. 3A, green cells). During early larval development, Wg signaling antagonizes EGF receptor signaling to specify identity of the wing pouch versus the notum. As a consequence, loss of Wg causes the conversion of wing into notum, whereas a gain of Wg induces the reciprocal conversion of notum into wing (26, 27). Wg also functions later in disk development to specify wing margin.

Misexpression of miR-315 in the wing disk by using the *ptc-Gal4* driver, which is active along the anterior–posterior compartment boundary, resulted in a dramatic double-wing pouch disk (Fig. 3B). The ectopic wing pouch expressed Nubbin and displayed features of a normally differentiating wing, including spatially appropriate expression of Cut, Wg, and Sens (Fig. 3B) (data not shown). The respecification of notum as wing

induced by ectopic miR-315 was quite similar to the effect of misexpressing Wg (Fig. 3C) (27), although it did not induce ectopic wing margin within the wing pouch proper, as seen with ectopic Wg (Fig. 3C, arrowhead).

Most *ptc-Gal4, UAS-DsRed-miR-315* animals died during early pupal development, but culturing at 18°C to minimize Gal4 activity permitted some to survive to pharate stages. Dissection of these animals from their pupal cases revealed transformations of scutellar tissue into ectopic wings (Fig. 3E and F), which is further evidence for the activation of Wg signaling by ectopic miR-315 *in vivo*.

miR-315 Directly Targets *Axin* and *Notum*, Essential Negative Regulators of the Wg Pathway. Because miR-315 genetically activates Wg signaling and miRNAs generally function as negative regulators, we hypothesized that miR-315 might target one or more inhibitors of the Wg pathway. In searching for such targets, we paid particular attention to targets containing multiple, canonical, conserved seed matches in their 3' UTRs (i.e., that display continuous Watson–Crick matches to positions 2–8 from the 5' end of miR-315). Interestingly, two critical negative regulators of the Wg pathway satisfy these criteria, namely *Axin* and *Notum* (Fig. 4A) (16, 17). These candidate targets contain a pair of miR-315 seed matches. One of the *Notum* sites and both of the *Axin* sites have been nearly perfectly conserved in all sequenced *Drosophilids* (Fig. 4A and SI Fig. 5). We also note that both *Axin* sites exhibit t1A features, which have been suggested to increase target activity (28). The sequenced *Drosophilids* preserve t1A features in both *Axin* sites.

Axin plays an integral role in the destruction of β -catenin in the absence of Wg signaling (29), whereas *Notum* (also known as Wingful) is a member of the α/β -hydrolase superfamily that negatively regulates Wg signal reception by modifying the cell-

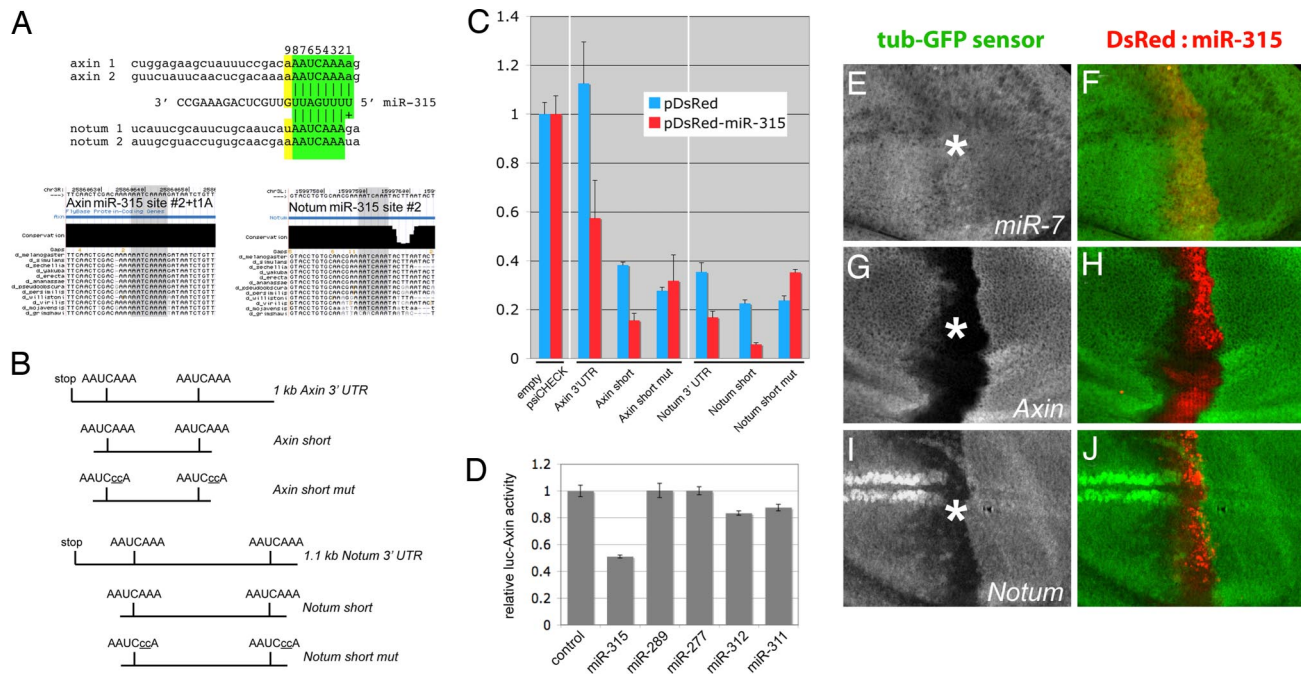


Fig. 4. miR-315 directly targets two negative regulators of the Wg pathway. (A) *Axin* and *Notum* each contain a pair of conserved seed matches to miR-315 (AAUCAAA, green shading). Both *Axin* sites are of the t1A variety, and all four sites exhibit t9W (i.e., A or U at position 9 of the miRNA, yellow) (28). (B) Schematic of wild-type and mutant 3' UTRs tested for responsiveness to miR-315. Full-length 3' UTR constructs include the sequence from the stop codon to ≈ 200 nt downstream of the annotated polyadenylation signal. (C) Assays of *Renilla*-luciferase-3' UTR sensor constructs cloned into psiCHECK2. S2 cells were cotransfected with a firefly/*Renilla* luciferase sensor, ub-Gal4, and either UAS-DsRed or UAS-DsRed-miR-315. The ratio of *Renilla*:firefly activity for each series was normalized to the response of the empty psiCHECK2 sensor, whose baseline ratio was set to 1. Ectopic miR-315 repressed wild-type full-length and short sensors for *Axin* and *Notum*, but mutant constructs containing point mutations in the miR-315 seed matches were immune to miR-315. (D) Other miRNAs with computationally predicted target sites in the *Axin* 3' UTR failed to regulate the *Axin* sensor. (E–J) Wing disk sensor assay. (Left) GFP expression in gray scale. (Right) Merge of GFP and DsRed. (E–J) Cells that express UAS-DsRed-miR-315 under the control of *ptc-Gal4* did not affect the expression of a control *tub-GFP* sensor containing miR-7-binding sites (E and F), but strongly inhibited sensors fused to the 3' UTRs of *Axin* (G and H) and *Notum* (I and J). Repression of GFP-*Axin* was stronger than that of GFP-*Notum*, which is consistent with the fact that both *Axin* target sites are of the t1A variety.

surface proteoglycans, Dally and Dlp (30, 31). To ask whether miR-315 could directly repress *Axin* or *Notum* by the candidate-binding sites present in their 3' UTRs, we constructed heterologous reporters (sensors) consisting of the *Renilla* luciferase gene fused to the entire *Axin* or *Notum* 3' UTRs. Coexpression with miR-315 resulted in >2 -fold repression of both *Axin* and *Notum* sensors (Fig. 4 B and C). We also assayed truncated sensors consisting of 3' UTR segments bounded by the miR-315 sites in each target and found that they recapitulated the quantitative repression by miR-315 mediated by their full-length counterparts. Finally, we introduced two point mutations into each of the miR-315 seed matches of the *Axin* and *Notum* sensors. These specific mutations abolished the response of these sensors to miR-315 (Fig. 4 B and C). Therefore, miR-315 directly represses *Axin* and *Notum* by the identified seed-match target sites.

As a more biologically relevant test, we assayed the ability of miR-315 to inhibit transgenic *Axin* and *Notum* sensors consisting of *tubulin-GFP* fused to their 3' UTRs. Expression of the GFP sensor was monitored in wing discs that express UAS-DsRed-miR-315 under the control of *ptc-Gal4*. As a control, we showed that expression of miR-315 had no effect on the activity of a *tub-GFP-miR-7* transgene (Fig. 4 E and F) previously shown to be strongly inhibited by ectopic miR-7 (23). In contrast, both GFP-*Axin* and GFP-*Notum* sensors exhibited strong, cell-autonomous inhibition in DsRed/miR-315-positive cells (Fig. 4 G–J). These transgenic tests provide compelling evidence that both target genes can be directly and potently repressed by miR-315 in the animal. We also note that the *Axin* sensor was

repressed more strongly than the *Notum* sensor, correlating with the t1A features in both *Axin* target sites.

Notum and Axin Are both Critical Functional Targets of miR-315 with Respect to Wg Signaling. The sensor data validated the ability of miR-315 to repress *Notum* and *Axin*, but did not directly assess how their repression contributes to miR-315-induced phenotypes. Therefore, we asked whether the effects of ectopic miR-315 could be suppressed by coactivation of its targets. Activation of endogenous *Notum* (by UAS sites integrated into this locus in the *EP-Notum* allele) by using *ptc-Gal4* resulted in complete embryonic lethality (0% hatching of $>1,000$ embryos). Coexpression with miR-315 suppressed the embryonic lethality of *ptc>Notum* animals, functional evidence that miR-315 can directly inhibit endogenously expressed *Notum* transcripts. Wing discs derived from *ptc>miR-315+Notum* animals also exhibited significant suppression of the notum-to-wing transformation normally induced by miR-315 (Fig. 3D). Further, 100% of *ptc>miR-315* discs ($n = 11$) exhibited a clearly duplicated wing pouch with a Nubbin⁺ domain at least half the size of the normal wing pouch (and typically approaching the size of the endogenous wing pouch). In contrast, coexpression of miR-315 and *Notum* resulted in only 50% ($n = 12$) of discs with evidence of a transformed wing pouch with ectopic Nubbin staining. Therefore, ectopic *Notum* can reciprocally rescue a mutant phenotype induced by ectopic miR-315.

We also tested for genetic suppression by *Axin*. When expressed by using *ptc-Gal4*, UAS-*Axin-GFP* induced embryo lethality in the absence or presence of coexpressed miR-315, so we could not examine wing discs in this genotype. We developed

previously (34). Dual-glo luciferase (Promega, Madison, WI) was used to measure the relative firefly and *Renilla* luciferase levels. Luciferase activity was measured on an analyst HT plate reader (Molecular Devices, Sunnyvale, CA).

For RNAi epistasis tests, dsRNAs were made and transfected as described (34). dsRNAs were selected from the DRSC collection on the basis of few, if any, predicted off targets and lack of CAR/CAN repeats (35). Their DRSC identification numbers are as follows: *arm* (DRSC18738), *wg* (DRSC03636), *dTCF* (DRSC17176), *legless* (DRSC17152), *arr* (DRSC07451), and *fz* (DRSC11348).

For luciferase sensor tests, wild-type and mutant *Axin* and *Notum* 3' UTRs were amplified from Canton S genomic DNA, cloned into pENTR (Invitrogen, Carlsbad, CA), and transferred into the XhoI and NotI sites of psiCHECK2 (Promega). Full-length sensors consist of genomic segments starting with the stop codon and extending to ≈ 200 nt downstream of the annotated polyadenylation signal into tub-GFP. Short sensors consist of the 3' UTR region bounded by the pair of miR-315 sites in each gene. Short mutant sensors contain AA \rightarrow CC point mutations in the miR-315 seed matches. Primers are as follows: notum full length, CACctcgag-TAGgctcaccacaaataccctg and cccgcggccgcTTTGCATATAAT-TATTTTGTTCGG; notum short, CACctcgagCATTTATTCAT-TCCGATTCTGCAATC and cccGCGGCCGCaagtaTTTGAT-Tttcgttcagc; notum short mut, cactcgcagCATTTATTCATTCG-CATTCTGCAATCaATCccAGaatgaaate and cccGCGGCCGCaagtaTggGATTtctgttcagcaggtac; axin full length, CACctcgagTAAattaagcatttagcgtag and cccgcggccgcAGATGTACA-ACATGAAGGCC; axin short, CACctcgagCAACTGGAGA-AGTATTTCCGAC and cccGCGGCCGcagattatcTTTT-GATTTTTgtc; and axin short mut, cactcgaGCAACTGGA-GAAGTATTTCCGACaAATCccAAgctatatg and CCCGC-GGCCGcagattatcTTggGATTtctgtcagttgaatg.

Drosophila Strains. For *Axin* and *Notum* transgenic sensors, we cloned the full-length 3' UTR and downstream genomic segments described into tub-GFP (23). *UAS-DsRed-miR-315* flies were generated by using the same construct used for tissue culture studies. Transgenic strains were made by BestGene Inc. (Chino Hills, CA) according to standard methods. *tub-GFP-miR-7* sensor was a kind gift of Stephen Cohen (Temasek,

Singapore) (23). The *UAS-Axin-GFP* transgene, the EP-*Notum* insertion, and the alleles *Axin*^{S044230}, *Wingful*¹⁴¹, *Notum*³, and *Notum*⁵ have all been described previously (30, 31, 36). Other publicly available strains were obtained from the Bloomington Stock Center (37), including *bx*^{MS1096}-*Gal4*, *ptc-Gal4*, *dpp*^{40C.6}-*Gal4*, and *UAS-wg*.

Immunohistochemistry. We performed immunostaining according to standard methods (38) by using the following primary antibodies: mouse α -Nubbin (1:50; gift of Stephen Cohen), mouse α -Cut (1:100; Developmental Studies Hybridoma Bank), mouse α -Wg (1:20; Developmental Studies Hybridoma Bank), guinea pig α -Sens (1:2,000; gift of Hugo Bellen, Baylor University, Houston, TX), and rabbit α -GFP (1:1,250; Molecular Probes). Native DsRed activity was detected. Secondary antibodies were Alexa 488 α -rabbit (1:600), Alexa 488 α -guinea pig (1:600), and Alexa 647 α -mouse (1:600), all from Molecular Probes. Processed discs were counterstained with Hoechst, mounted in Vectashield (Vector Laboratories, Burlingame, CA), and analyzed on an Axioimager Z1 fitted with Apotome (Carl Zeiss, Thornwood, NY).

We thank Bergin Tam and David Raleigh for assistance with construction of the miRNA expression library; Kent Nybakken (Harvard Medical School, Boston, MA) (Hh), Ram Dasgupta (New York University, New York, NY) (Wg), and Rui Chen (Harvard Medical School, Boston, MA) (JAK/STAT) for cell-based assay plasmids; Hugo Bellen, Konrad Basler (Universität Zürich, Zürich, Switzerland), Nick Tolwinski (Sloan-Kettering Institute, New York, NY), and Stephen Cohen for serum antibodies and fly strains; Nancy Arango for cloning the GFP-*Axin* and GFP-*Notum* sensors; Eric Joseph for initial characterization of the *UAS-DsRed-miR-315* transgene; the DRSC for dsRNA templates and use of their plate reader; and Gerald Rubin for logistical support during the early phases of this work. This work was supported by the Developmental Studies Hybridoma Bank (Iowa City, IA) under the auspices of the National Institute of Child Health and Human Development, a Damon Runyon Cancer Research Foundation Fellowship (to S.J.S.), a Mildred and Emil Holland Scholarship (to J.W.H.), a Margaret and Herman Sokol Fellowship, and National Institutes of Health Grant GM07739. N.P. is an investigator of the Howard Hughes Medical Institute, and E.C.L. is a fellow of the Leukemia and Lymphoma Society, the Burroughs Wellcome Foundation, the V Foundation for Cancer Research, and the Sidney Kimmel Cancer Foundation.

- Lai EC (2003) *Curr Biol* 13:R925–R936.
- Rajewsky N (2006) *Nat Genet* 38(Suppl 1):S8–S13.
- Johnson SM, Grosshans H, Shingara J, Byrom M, Jarvis R, Cheng A, Labourie E, Reinert KL, Brown D, Slack FJ (2005) *Cell* 120:635–647.
- Mayr C, Hemann MT, Bartel DP (2007) *Science* 315:1576–1579.
- Lee YS, Dutta A (2007) *Genes Dev* 21:1025–1030.
- Shell S, Park SM, Radjabi AR, Schickel R, Kistner EO, Jewell DA, Feig C, Lengyel E, Peter ME (2007) *Proc Natl Acad Sci USA* 104:11400–11405.
- Voorhoeve PM, le Sage C, Schrier M, Gillis AJ, Stoop H, Nagel R, Liu YP, van Duijse J, Drost J, Griekspoor A, et al. (2006) *Cell* 124:1169–1181.
- He L, Thomson JM, Hemann MT, Hernando-Monge E, Mu D, Goodson S, Powers S, Cordon-Cardo C, Lowe SW, Hannon GJ, Hammond SM (2005) *Nature* 435:828–833.
- O'Donnell KA, Wentzel EA, Zeller KI, Dang CV, Mendell JT (2005) *Nature* 435:839–843.
- Flynt AS, Li N, Thatcher EJ, Solnica-Krezel L, Patton JG (2007) *Nat Genet* 39:259–263.
- Lai EC, Burks C, Posakony JW (1998) *Development (Cambridge, UK)* 125:4077–4088.
- Lai EC, Posakony JW (1997) *Development (Cambridge, UK)* 124:4847–4856.
- Lai EC, Tam B, Rubin GM (2005) *Genes Dev* 19:1067–1080.
- Clevers H (2006) *Cell* 127:469–480.
- DasGupta R, Kaykas A, Moon RT, Perrimon N (2005) *Science* 308:826–833.
- Stark A, Brennecke J, Bushati N, Russell RB, Cohen SM (2005) *Cell* 123:1133–1146.
- Grun D, Wang Y-L, Langenberger D, Gunsalus KC, Rajewsky N (2005) *PLoS Comp Biol* 1:51–63.
- Enright AJ, John B, Gaul U, Tuschl T, Sander C, Marks DS (2003) *Genome Biol* 5:R1.
- Long D, Lee R, Williams P, Chan CY, Ambros V, Ding Y (2007) *Nat Struct Mol Biol* 14:287–294.
- Didiano D, Hobert O (2006) *Nat Struct Mol Biol* 13:849–851.
- Korinek V, Barker N, Willert K, Molenaar M, Roose J, Wagenaar G, Markman M, Lamers W, Destree O, Clevers H (1998) *Mol Cell Biol* 18:1248–1256.
- Barolo S (2006) *Oncogene* 25:7505–7511.
- Stark A, Brennecke J, Russell RB, Cohen SM (2003) *PLoS Biol* 1:E60.
- Griffiths-Jones S, Grocock RJ, van Dongen S, Bateman A, Enright AJ (2006) *Nucleic Acids Res* 34:D140–D144.
- Hutvagner G, Simard MJ, Mello CC, Zamore PD (2004) *PLoS Biol* 2:e98.
- Wang SH, Simcox A, Campbell G (2000) *Genes Dev* 14:2271–2276.
- Ng M, Diaz-Benjumea FJ, Vincent JP, Wu J, Cohen SM (1996) *Nature* 381:316–318.
- Lewis BP, Burge CB, Bartel DP (2005) *Cell* 120:15–20.
- Tolwinski NS, Wieschaus E (2001) *Development (Cambridge, UK)* 128:2107–2117.
- Giraldez AJ, Copley RR, Cohen SM (2002) *Dev Cell* 2:667–676.
- Gerlitz O, Basler K (2002) *Genes Dev* 16:1055–1059.
- Lindsley DL, Sandler L, Baker BS, Carpenter ATC, Denell RF, Hall JC, Jacobs PA, Miklos GL, Davis BK, Gethman RC, et al. (1972) *Genetics* 71:157–184.
- Baeg GH, Zhou R, Perrimon N (2005) *Genes Dev* 19:1861–1870.
- Nybakken K, Vokes SA, Lin TY, McMahon AP, Perrimon N (2005) *Nat Genet* 37:1323–1332.
- Kulkarni MM, Booker M, Silver SJ, Friedman A, Hong P, Perrimon N, Mathey-Prevot B (2006) *Nat Methods* 3:833–838.
- Hamada F, Tomoyasu Y, Takatsu Y, Nakamura M, Nagai S, Suzuki A, Fujita F, Shibuya H, Toyoshima K, Ueno N, Akiyama T (1999) *Science* 283:1739–1742.
- Grumbling G, Strelets V (2006) *Nucleic Acids Res* 34:D484–D488.
- Lai EC, Rubin GM (2001) *Dev Biol* 231:217–233.